



STUDYING THE PERFORMANCE OF MICROPILED SYSTEM IN SANDY SOIL SUBJECTED TO VERTICAL LOADS FOR IMPROVING BEARING CAPACITIES

Eslam Hassan^{1,*}, Hussein Mostafa², Wagdy El Banna³, Mohamed Rabie⁴

¹ Assistant lecturer, Faculty of Engineering at Mataria branch, Helwan University, Cairo, Egypt

² Lecturer, Faculty of Engineering at Mataria branch, Helwan University, Cairo, Egypt

³ Lecturer of Geotechnical Engineering, 15th May Institute in Cairo, Egypt

⁴ Professor of Geotechnical Engineering, Faculty of Engineering at Mataria branch, Helwan University, Cairo, Egypt

*Corresponding author E-mail: Eslam.ahmed2020@m-eng.helwan.edu.eg

Abstract. Micropiles are grouted piles with a small diameter. The bond between the grout and the surrounding ground depends on the grouting method. Type A as mentioned in FHWA 2005 is one of the common type of these methods that grout is placed under gravity head only. This technique is the most suitable for experimental work. This study explores the axial behavior and load-carrying capacity of micropiles in sand under vertical loading, highlighting the effects of the slenderness ratio (L/D) and water-to-cement (W/C) ratio on performance. The results demonstrate that micropiles with higher slenderness ratios (e.g., $L/D = 14$) and lower W/C ratios (e.g., 0.3) exhibit superior load-bearing capacity. Specifically, $W/C = 0.3$ achieved maximum loads exceeding 5886 N, while higher ratios ($W/C = 0.55$) significantly reduced strength and stiffness due to weaker grout properties. A mathematical model was developed to predict pile load capacity based on deflection, L/D ratio, and W/C ratio, providing a practical tool for optimizing pile design. This research emphasizes the importance of geometric properties and grout composition in enhancing micropile efficiency under various loading conditions. The validation of the model used was vitrified with another model (Binu Sharma 2014). Load – settlement for all tests cleared in the present paper. Equation of pile load determination was derived as function of deflection of pile, W/C ratio and slenderness ratio L/D .

Keywords: Micropile, Single pile, Pile capacity, Grout injection, Cohesionless soil.

1 Introduction

Micropiles are small-diameter, high-strength piles designed for foundation reinforcement and ground improvement. Since their invention over fifty years ago, micropiles have played a crucial role in addressing geotechnical challenges, particularly during post-war reconstruction efforts. Initially conceived as innovative solutions for supporting structures in complex conditions, micropile technology

has undergone significant advancements over the last two decades. The focus has shifted from utilizing networks of limited-capacity micropiles to employing individual high-capacity elements capable of handling heavy loads and accessing constrained spaces. Typically, micropiles are categorized as small-diameter deep foundations, with diameters ranging from 150 to 300 mm. One common construction method, referred to as Type [A], involves placing grout under gravity head without external pressure. This method utilizes sand-cement mortars or neat cement grouts to form the bond between the pile and the surrounding soil. These advancements have enabled micropiles to become essential tools for geotechnical engineers in managing complex foundation requirements.

Micropiles are constructed by placing a central reinforcing element and cement grout into a pre-drilled hole in the ground. The primary load transfer mechanism for micropiles is skin friction that develops between the grout and the surrounding soil in the bonded zone. This interaction transforms the soil into a cohesive composite mass capable of withstanding high compressive loads at defined settlement levels or supporting specific loads with minimal movement. Studies by [1] and [2] have shown that the engineering behavior of micropile-reinforced soils is significantly influenced by group effects (the collective interaction of multiple micropiles) and network effects (the interaction of micropiles with the surrounding soil matrix). These effects enhance the total resistance and shear strength of the composite system, making it a reliable solution for improving soil stability. Moreover, micropiles create an in situ coherent composite reinforced soil system, which combines the strengths of the soil and the reinforcing grout to achieve high performance under varying load conditions.

Juran et al. [3] submitted a comprehensive state-of-the-art review that addressed every study and contribution to the current state of micropile practice. A great deal of detail has been covered about the construction of individual micropiles, the assessment of load-bearing capability, movement estimate models, and the impact of group and network effects. The writers also looked at various nations' geotechnical design recommendations for axial and lateral load capacities as well as methods for estimating movement. Micropiles have been widely adopted for various engineering applications, such as underpinning existing foundations to support structures subjected to additional loads, controlling differential settlements and strengthening an existing building with problems as a result of bad exploration of the site before construction or unforeseen problems have occurred to the soil. Numerous scholars have documented the use of micropiles in soil reinforcing, retrofitting, and underpinning projects in their publications as [4][5],[6], [7], [8], [9], [10] and [11].

2 Experimental Work Description

This section outlines the experimental methodology employed to investigate the enhancement of single micropiles under vertical loads. The goal of the current study is to examine the axial behavior and capacities of this sort of pile in the sand under vertical loads using various factors, such as the grout's water-cement ratio; W/C and slenderness (pile length / pile diameter) ratio; L/D .

2.1 The Soil Container

According to theories and previous models of axially loaded piles. the soil container needs to be large enough so the container's edges will not affect the test results, as the zone of influence of the micropile due to loading. [12] indicated the influence zone under the pile that extended to 6 times the pile diameter from pile tip .[13] mentioned that the horizontal distance between the pile and the container boundaries should be 3-5 times the pile diameter. In relation to the dimensions of the micropile model, it was expected that these dimensions would be large enough to reduce the impact of the boundary on the test findings. The container measured 800 by 800 mm in plan and 700 mm in depth as shown in **Fig. 1**.



Fig. 1. The metal box (Container) for soil sample preparation.

2.2 Loading system

To apply the load, a mechanical jack system was used, where the jack was placed on a steel footing connected with the micropile head, a load cell was installed on the experimental frame touching with the head of the jack. Two dial gauges were used for settlement measurements. The loading was starting by using hand-arm slowly with a suitable rate and the load was recorded on a digital screen. The experimental setup and instrumentation are described in detail to provide a clear understanding of the experimental framework as shown in **Fig. 2**.



Fig. 2. Loading system for experimental work.

2.3 Micropile Model

Experimental tests of the single micropile model are performed on a hollow circular steel pipe with outer diameter 19 mm and inner diameter 17 mm. Grout needs to be pumpable in addition to having a high strength and stability (bleed). Type A [14] is the type used in the present study and it depends on that grout is placed under gravity head only and the cement grouts can be used. A drilling tool with the same diameter as the pipe was used, along with the use of bentonite liquid, and then the outer diameter became 37.5 mm as shown in **Fig. 3**. The pipes used in the tests were coated with anti-corrosion material to simulate field conditions.



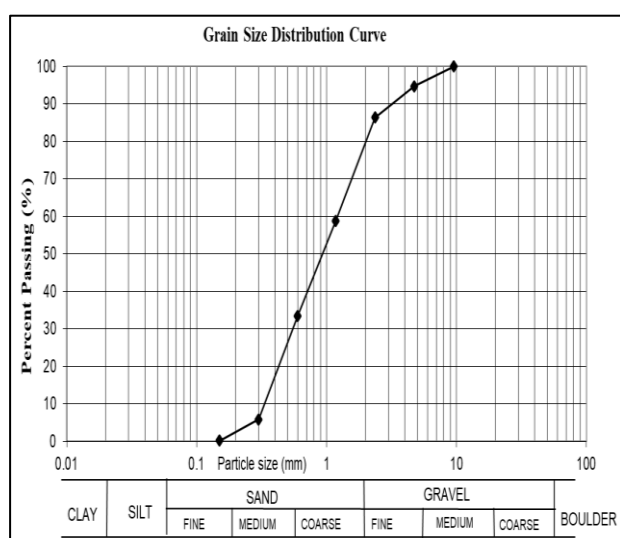
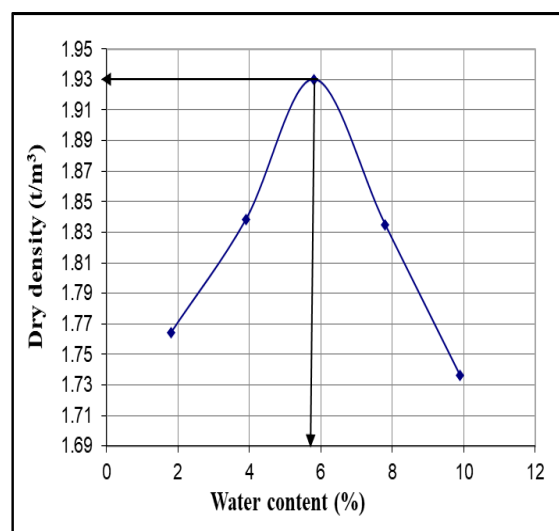
Fig. 3. Model micropile

2.4 Properties of Tested Soils

The axial behavior and capacities of this pile type in sand subjected to vertical loads were investigated in the current study using sandy soil, which is frequently needed in compaction works for construction purposes. Modified Proctor compaction tests were carried out in the laboratory for the sandy soil. **Table 1** summarizes the results obtained for the investigated soil including its constituents, classification, maximum dry density, and the corresponding optimum moisture contents. In addition, the obtained minimum dry density and the angle of shearing resistance are presented. **Fig. 4** and **Fig. 5** show the particle size distribution curves and the compaction curves for the tested soil. The used soil was uniformly compacted, with the same moisture content for all tests. It worth to mention that the tested soil is placed in the container in layers with the same compaction energy and moisture content.

Table 1. Physical and mechanical properties for the tested soil.

Parameter	Maximum dry unit weight	Minimum dry unit weight	Maximum void ratio	Minimum void ratio	Specific gravity	Gravel	Coarse sand	Medium sand	Fine sand	Effective diameter	USCS Classification	Water content	Friction angle
Symbol and unit	γ_{dmax} (gm/cm ³)	γ_{dmin} (gm/cm ³)	e_{max}	e_{min}	Gs	%	%	%	%	D ₁₀ (mm)	SP	O.M.C (%)	Φ (degree)
Value	1.93	1.72	0.52	0.36	2.62	13.6	52.9	33.3	0.21	0.34	-	5.8	38.3°

**Fig. 4.** Particle size distribution for the tested soil.**Fig. 5.** Compaction curves using the Modified Proctor test, for the SP soil.

3 Experimental Work Program

To comprehend micropile behavior, an experimental work program was carried out on the previously mentioned tested soil. The purpose of the laboratory test program was to examine the impact of various parameters as the slenderness ratio (L/D) and water–cement ratio (W/C) of grout. To evaluate the capacity of the micropile (type A), 9 tests were executed with changing L/D with 10, 12 & 14 and W/C of grout with 0.3, 0.4 & 0.55 as shown in the laboratory test program in **Table 2**. The slenderness ratio of a micropile significantly affects the pile's buckling. The choice of the mentioned slenderness ratios is to minimize the risk of buckling under compressive loads. In addition, these ratios provide a cost-effective solution compared to the high ratios due to the reduction in material volume. From the viewpoint of the behavioral analysis, the ratio of 10 focused on end-bearing and settlement, while 12 and 14 emphasized the load distribution and slenderness effects. Moreover, there are many researchers used these ratios (e.g; [15]). To ensure the practical relevance of our study, the water-cement ratios were selected based

on the recommendations outlined in the [14] guidelines. By choosing values of 0.3, 0.4, and 0.55, we were able to cover a representative range within the recommended limits, allowing us to systematically investigate the impact of W/C on the bearing capacity of the micropiles.

Table 2. The laboratory test program

Test No.	L(cm)	D(cm)	L/D	Dr (%)	W/C
1	37.5	3.75	10	90	0.4
2	37.5	3.75	10	90	0.3
3	37.5	3.75	10	90	0.55
4	45	3.75	12	90	0.4
5	45	3.75	12	90	0.3
6	45	3.75	12	90	0.55
7	52.5	3.75	14	90	0.4
8	52.5	3.75	14	90	0.3
9	52.5	3.75	14	90	0.55

4 Testing Procedure

The experimental testing procedure was divided into two phases, the first phase is the implementation of micropile, and the second phase comes next by loading the executed micropile. The first stage is summarized in the following steps:

1. Using a specialized drilling tool, a borehole is drilled to the predetermined depth. The diameter of the borehole is slightly larger than the micropile to allow for grout with the use of bentonite fluid. Bentonite was injected with a suitable drilling pump as shown in **Fig. 6**.
2. Then the grout is injected by the same pump until any remaining soil or bentonite liquid is removed from the hole as shown in **Fig. 7**.
3. At this stage, putting down the micropile is done as shown in **Fig. 8**.
4. Base plate is installed for loading preparation as shown in **Fig. 9**.

The second stage is summarized in loading the micropile, A mechanical hydraulic jack was utilized to apply the load at an approximately constant rate of 1 mm/min. Additionally, to ensure the uniformity of load distribution on the pile, a steel plate was used to transfer the load from the jack to the pile. Also, the contained and the loading steel plate were fixed enough to avoid any side vibrations.; a load cell was mounted on the experimental frame and made contact with the jack's head; measurement uncertainties and potential errors, including those related to settlement readings, were systematically addressed throughout the testing process. To mitigate these uncertainties, highly accurate and calibrated dial gauges were employed. Multiple readings were taken at each load increment to ensure consistency and reliability. Any discrepancies between individual readings were thoroughly analyzed, and average values were calculated to account for minor variations and enhance the overall accuracy of the data. Beginning with the loading of the hand arm at a reasonable pace, the load was displayed on a digital screen. To provide a thorough grasp of the experimental framework, a detailed description of the experimental setup and instrumentation is provided as shown in **Fig. 10**. After the test, no failure in the pipe itself was observed; and hence, the failure was directly related to micropile settlement.

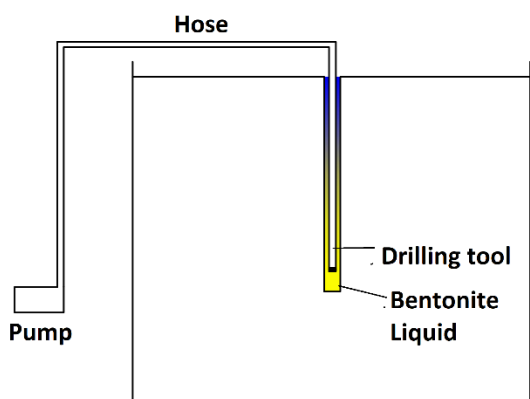


Fig. 6. Stage 1: Pumping Bentonite liquid

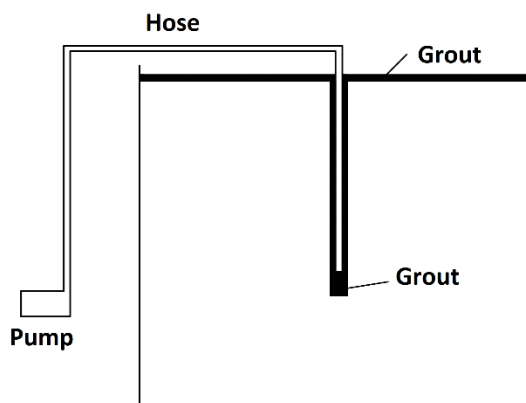


Fig. 7. Stage 2: Pumping Grout

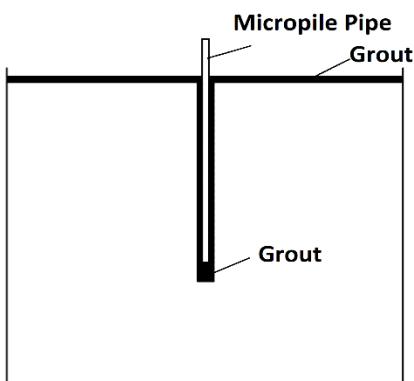


Fig. 8. Stage 3: Putting down the micropile

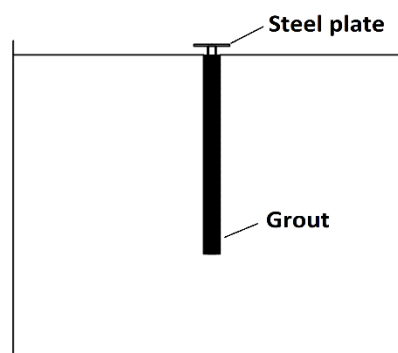


Fig. 9. Stage 4: Steel plate installation

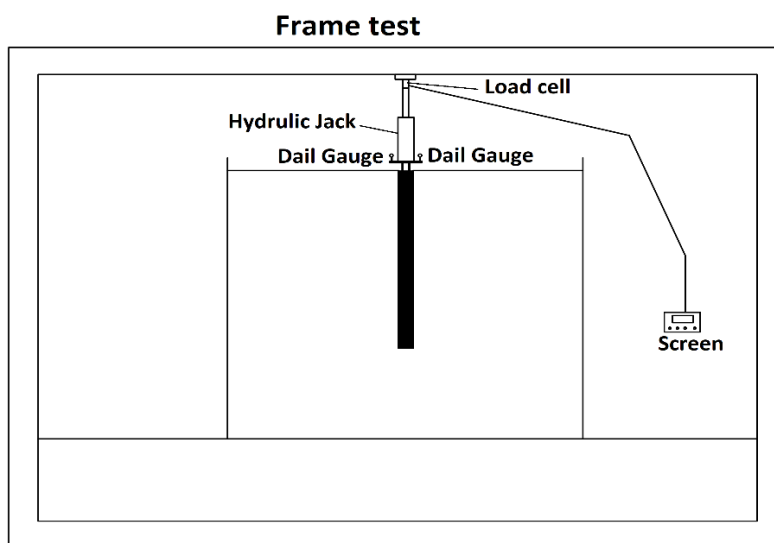


Fig. 10. Stage 5: Loading

5 Testing Results

Compression loading experiments on a single micropile model implanted in sand soil make up the majority of the test program. The load-settlement relationship was used to calculate the ultimate micropile capacity and the corresponding vertical displacement of failure, which is the point at which the curve peaks or continues to increase in displacement while the micropile resistance does not increase any further. **Figs. 11, 12 and 13** show the load-displacement relationship for the micropile with slenderness ratios L/D of 10, 12 and 14 at water-cement ratios W/C of 0.3, 0.4 and 0.55. The results of the micropile loading at last three figures show that the micropile capacity increases by increasing slenderness ratio L/D , Also the results show that the micropile capacity decreases by increasing water cement ratio W/C .

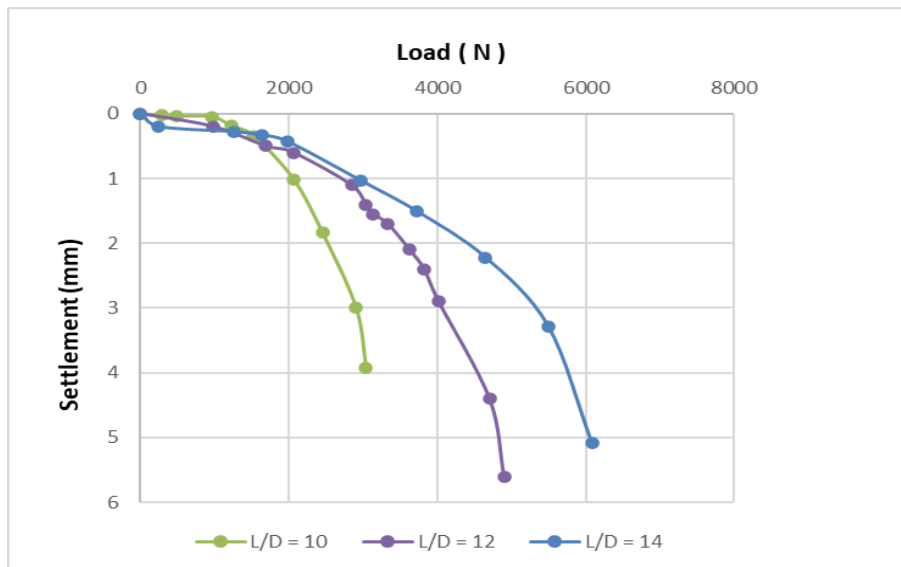


Fig. 11. Load-Settlement relationship for $L/D = 10, 12$ & 14 at $W/C = 0.3$

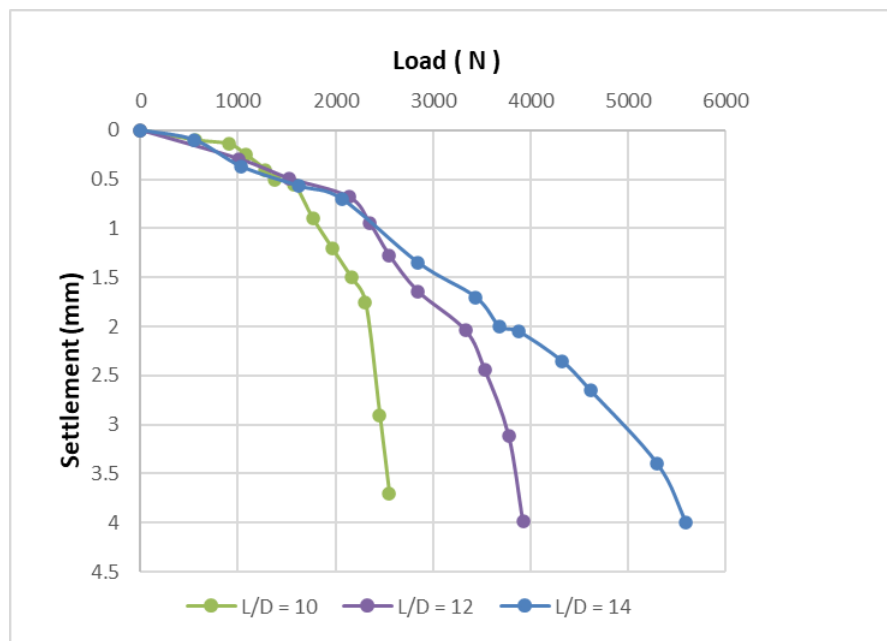


Fig. 12. Load-Settlement relationship for $L/D = 10, 12$ & 14 at $W/C = 0.4$

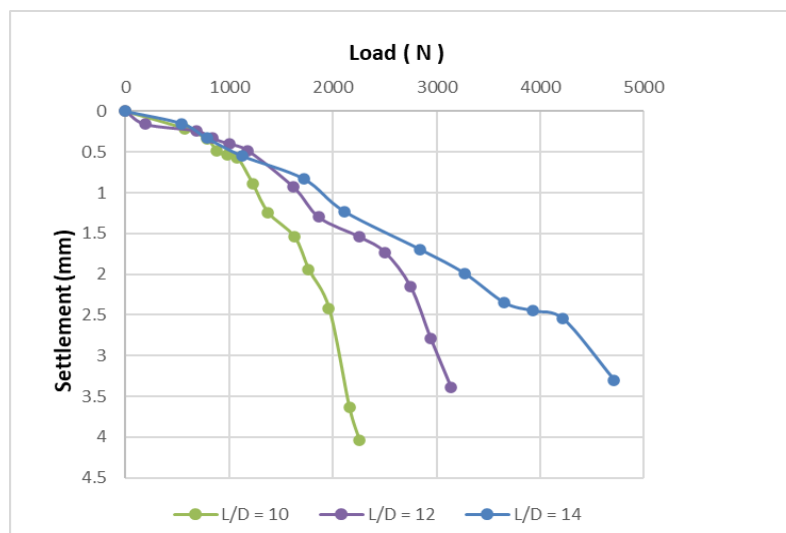


Fig. 13. Load-Settlement relationship for L/D = 10, 12 & 14 at W/C = 0.55

6 Verification

To validate the findings of the present study, a comparison was made with the results of a previous experimental study conducted by Binu Sharma. [15] presented the findings of an experimental investigation carried out to comprehend how vertical and damaged micropiles with varying length/diameter ratios (L/D) would react to lateral and vertical stress conditions. With a growing L/D ratio, it was discovered that the vertical load carrying capacity rose. Installed in the model tank and loaded vertically was a model consisting of forty micropiles with four distinct batter angles and ten various length-to-diameter ratios (L/D) (12, 18, 24, 30, 36, 42, 48, 56, 62, and 68). This study, which focused on similar parameters such as slenderness ratio (L/D) of 12, 24 and 36, water-cement ratio (W/C) of 0.5, and sand relative density of 50%, provided a reliable benchmark for assessing the accuracy of the experimental data collected in this research. A comparison was made with 3 experiments and involved analyzing key performance metrics, including load-settlement behavior, and evaluating how closely the results align with those reported in the referenced study. **Fig. 14** shows the load-settlement relationship for the micropile pile of 12, 24 & 36 slenderness ratio. It's worth noting that the experimental setup in this study was designed to closely replicate the conditions in Sharma's study, particularly in terms of relative density, soil type, and W/C ratio of grout, to ensure a meaningful comparison. The primary objective of the comparison with Binu Sharma's study was to validate the experimental model employed in this research. While we realize that differences in soil conditions, pile dimensions, and testing protocols may have contributed to discrepancies, the overall trend of the results supports the model's accuracy. A more in-depth parametric study, considering a wider range of variables, would be necessary to fully explore the effects of L/D ratio on settlement behavior and to address the apparent contradiction regarding buckling susceptibility. However, this was beyond the scope of the current study.

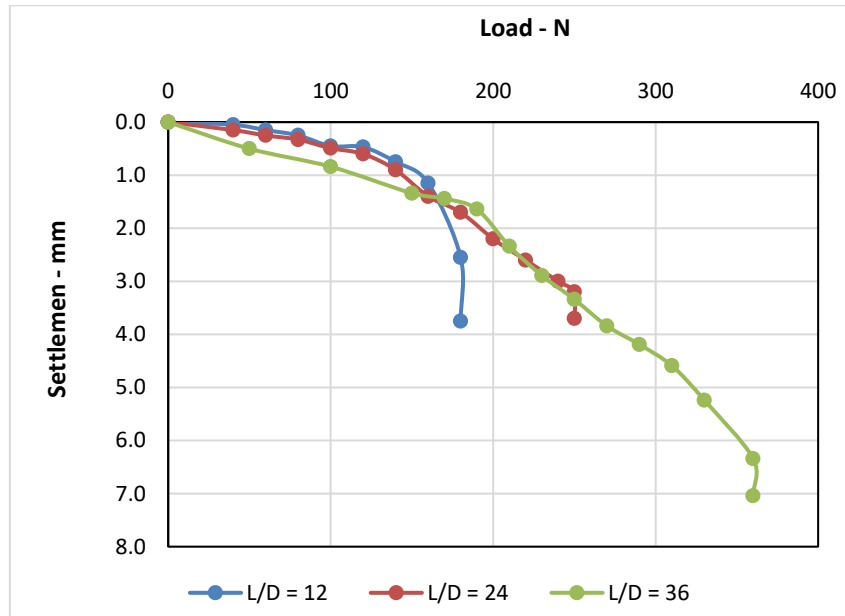


Fig. 14. Load- Settlement relationship For L/D = 12, 24 & 36 (For Validation)

The close correlation between the findings from both studies enhances the validity of the research and demonstrates the robustness of the experimental methodology employed. This validation step confirms that the conclusions drawn from this work are consistent with established research in the field. **Figs. 15 and 16** show the comparison of load–settlement relationship between the present study and Binu Sharma study.

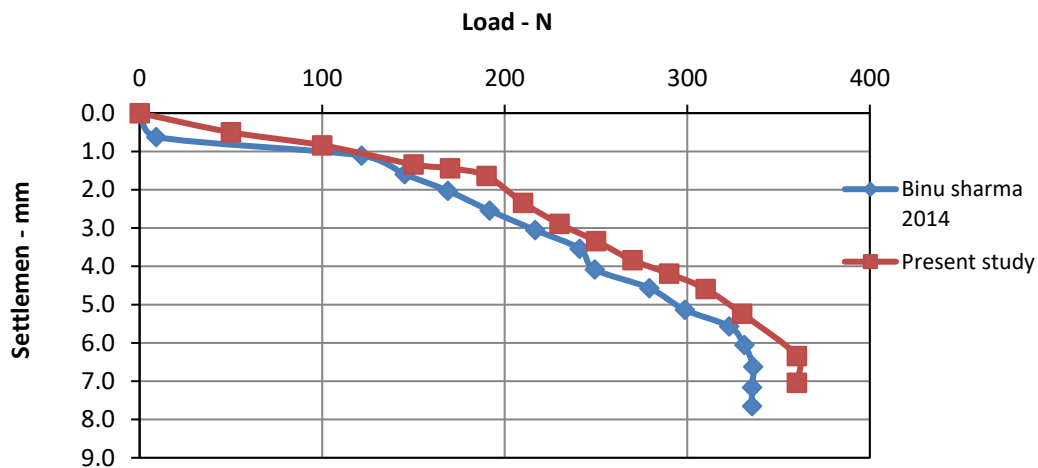


Fig. 15. Comparison of the load-settlement relationship between present and Sharma studies (L/D = 36)

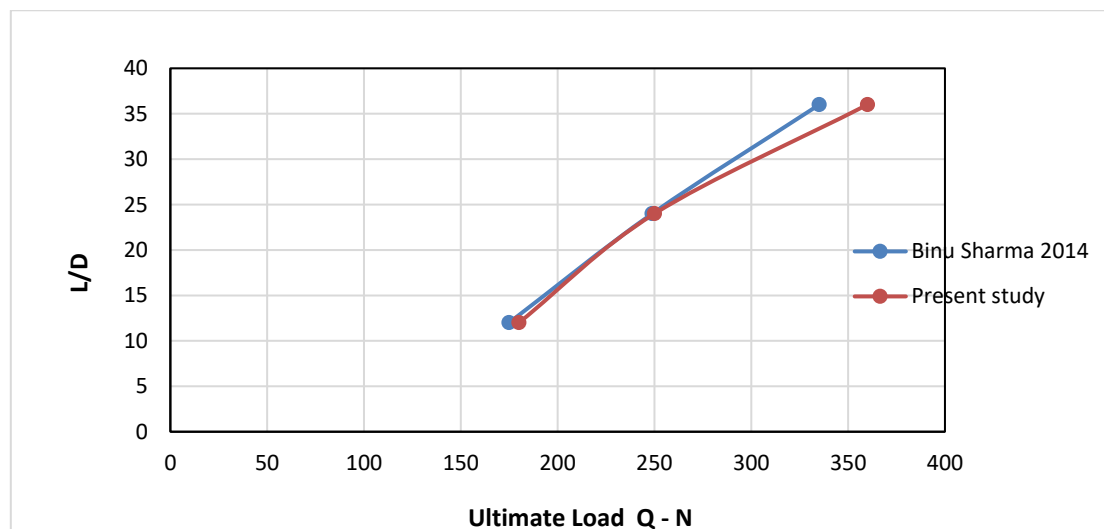


Fig. 16. Comparison L/D & ultimate load relationship between present and Sharma studies

7 Results analysis

7.1 Analysis of the results

Based on the provided graphs, we can make the following observations:

Effect of Slenderness Ratio:

- As the slenderness ratio increases (from 10 to 12 to 14), the load-carrying capacity of the micropile generally decreases. This is because slenderer piles are more susceptible to buckling under load.
- The initial stiffness of the pile (slope of the curve at low loads) also tends to decrease with increasing slenderness ratio, indicating a reduction in resistance to small deformations.
- As the slenderness ratio increases, the load-bearing capacity increases, especially at the micropile with $L/D = 14$ which shows the highest load capacity.

Effect of Water-Cement Ratio:

- A higher water-cement ratio (W/C) generally results in a lower load-carrying capacity of the micropile. This is because a higher W/C ratio leads to weaker injected grout, which is less able to resist compressive stresses.

Overall Trend:

- The maximum settlement is ranging from approximately 0 to 4 mm.
- The load-settlement curves exhibit a typical nonlinear behavior, with the initial portion being relatively stiff and the latter portion showing a more gradual increase in settlement with increasing load.
- The point at which the curve starts to show a significant increase in settlement is often referred to as the ultimate load or failure load of the pile.
- The trends observed in this study are consistent with geotechnical principles. Higher slenderness ratios improve load distribution through increased skin friction but require careful design to

prevent buckling. Lower W/C ratios enhance grout strength and stiffness, resulting in better performance, while higher ratios lead to weaker bonds and greater settlement. These insights are critical for optimizing micropile design to balance load capacity, structural stability, and cost-effectiveness.

A common definition of a micropile's ultimate load capacity is a load equal to 10% of the micropile diameter, which corresponds to settlement. Because of its smaller size and function as a foundation underpinning for existing foundations, a micropile makes it difficult to determine the settlement level for the ultimate load capacity. [16]and [17]used the Davission's criterion [18] to define the ultimate load carrying capacity of micropiles, which would produce a conservative load-carrying capacity. [19]and [20]used the intersection method to find a load that intersects the initial and final tangent lines on load-settlement curve. **Table 3** shows the ultimate capacity of micropile and capacity at 10 % of micropile diameter.

Table 3. The laboratory test program

Test No.	L/D	W/C	Ultimate Capacity - N	Ultimate capacity at 10% D - N
1	10	0.3	3041	2972
2	12	0.3	4905	4797
3	14	0.3	6082	6004
4	10	0.4	2551	2374
5	12	0.4	3924	3953
6	14	0.4	5592	5464
7	10	0.55	2256	2207
8	12	0.55	3139	3002
9	14	0.55	5003	4934

7.2 Derivation of a mathematical model

The behavior of micropiles under loading is influenced by various factors such as the pile's slenderness ratio (L/D) and the water–cement ratio (W/C) of the concrete used. Understanding the relationship between these variables and the resulting load (Q) and vertical displacement (d) is essential for optimizing pile design. This study aims to derive an empirical equation that connects these variables using experimental and theoretical data.

Experimental data were collected from pile load tests conducted on micropiles with varying slenderness ratios and water–cement ratios. These tests measured the applied load and corresponding vertical displacement. Through regression analysis and numerical modeling using **Colab Google**, an equation was derived to express the relationship between these variables.

Based on the data, the relationship between the load (Q), displacement (d), W/C ratio, and L/D ratio was found to be non-linear. The following general form of the equation was developed:

$$Q = [-94.12 - 18.89 * d + 39.18 * \left(\frac{L}{D}\right) - 176.23 * \left(\frac{W}{C}\right) - 23.18 * d^2 - 1.8 * \left(\frac{L}{D}\right)^2 + 20.13 * d * \left(\frac{L}{D}\right) - 88.29 * d * \left(\frac{W}{C}\right)] * 9.81$$

Where ;

Q : The load on pile – N .

d : Vertical deflection of pile – mm .

L/D : The slenderness ratio of micropile.

W/C : The ratio of water weight to cement weight.

Analysis of the Equation:

- The constant (-94.12) provides a baseline load value, accounting for the overall stiffness and properties of the pile-soil system.
- The term (-18.89d) shows a direct inverse relationship between vertical deflection and load, where an increase in deflection generally leads to a reduction in load capacity.
- The term $39.18(L/D)$ indicates that a higher slenderness ratio increases the load capacity, as longer piles are more effective at distributing the applied load.
- The term $-176.23(W/C)$ reflects the significant negative impact of higher water-to-cement ratios on the pile's load capacity. As W/C increases, the concrete becomes weaker, reducing the overall strength and load-bearing ability of the pile.
- The second-order terms $-23.18d^2$ and $-1.8(L/D)^2$ capture the non-linear effects of deflection and slenderness ratio on the load, providing more accuracy in predicting load behavior, particularly at extreme values.
- The interaction terms $20.13d(L/D)$ and $-88.29d(W/C)$ highlight the combined influence of deflection with slenderness ratio and water-to-cement ratio, showing that these factors do not act independently but rather interact to influence the load capacity of the pile.

Figs. 17 to 25 show verification of the equation with the results of experimental work.

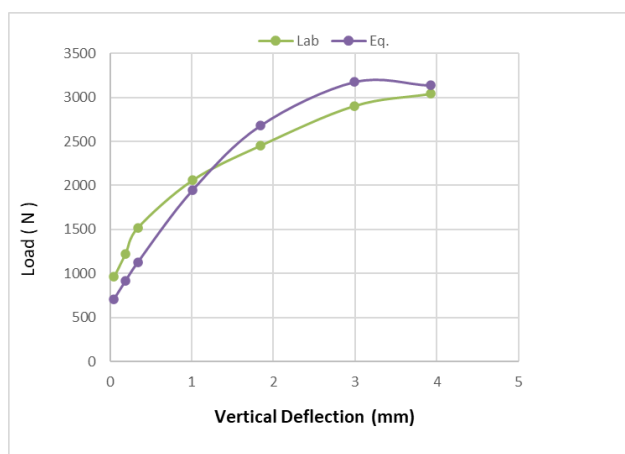


Fig. 17. Comparison between Derived equation & Experimental results – Test 1

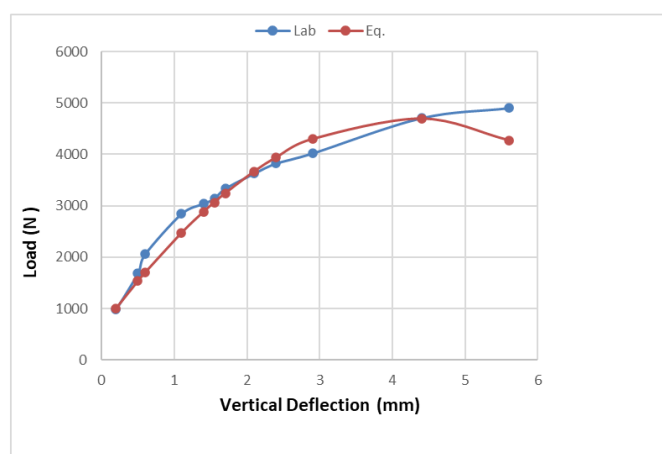


Fig. 18. Comparison between Derived equation & Experimental results – Test 2

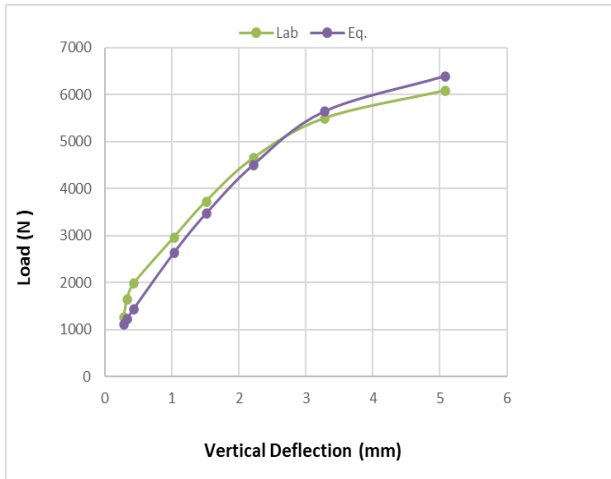


Fig. 19. Comparison between Derived equation & Experimental results – Test 3

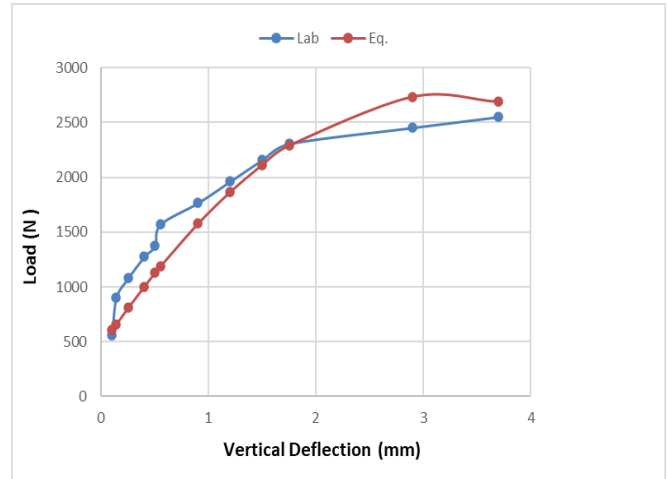


Fig. 20. Comparison between Derived equation & Experimental results – Test 4

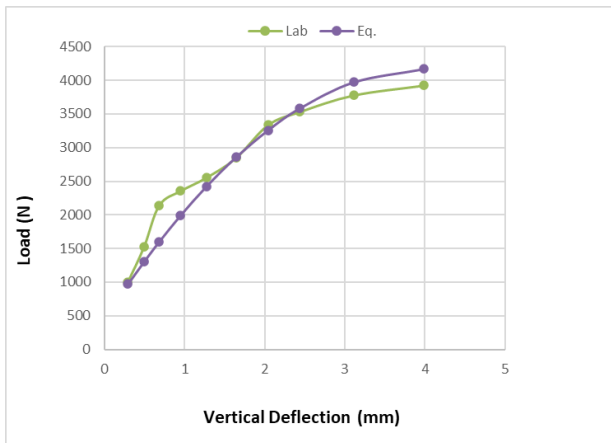


Fig. 21. Comparison between Derived equation & Experimental results – Test 5

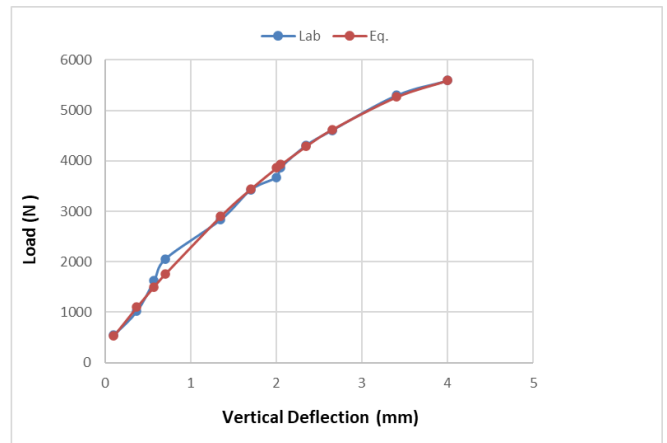


Fig. 22. Comparison between Derived equation & Experimental results – Test 6

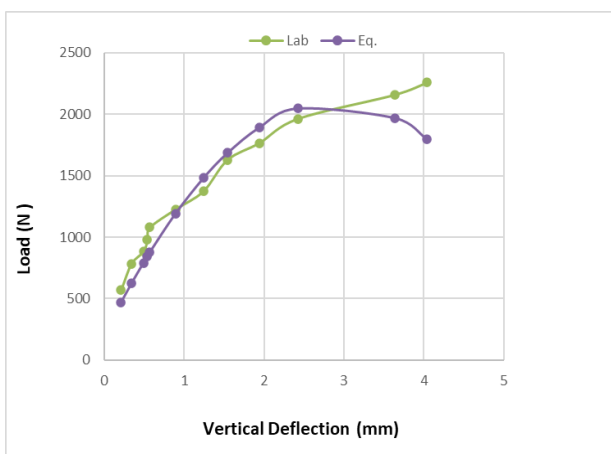


Fig. 23. Comparison between derived equation & Experimental results – Test 7

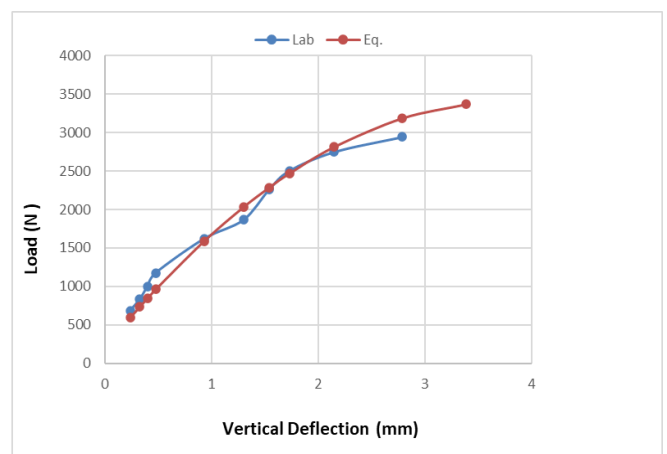


Fig. 24. Comparison between derived equation & Experimental results – Test 8

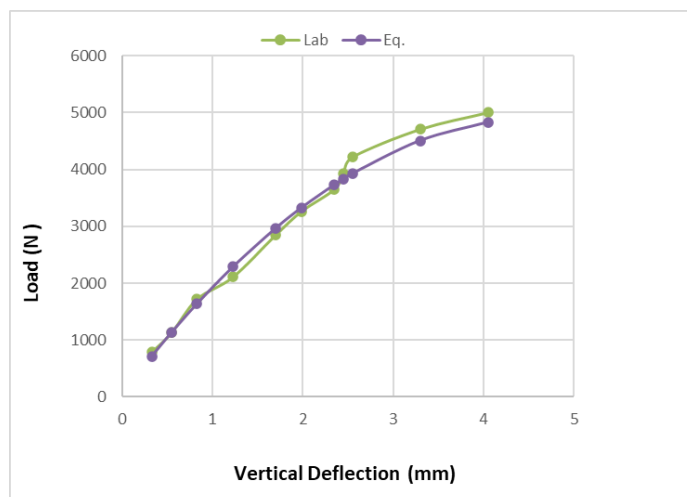


Fig. 25. Comparison between Derived equation & Experimental results – Test 9

8 Conclusions

The findings of this investigation can be summed up as follows:

1. Impact of Slenderness Ratio (L/D):

- Across all three water–cement ratios ($W/C = 0.3$, $W/C = 0.4$, and $W/C = 0.55$), the slenderness ratio has a significant influence on the load-bearing capacity of the micropile.
- The slenderness ratio $L/D = 14$ consistently shows the highest load-carrying capacity at each level of vertical deflection. This indicates that piles with a higher slenderness ratio (longer piles relative to their diameter) are able to sustain larger loads, as they distribute the load more effectively into the surrounding soil.
- The slenderness ratio $L/D = 10$ exhibits the lowest load capacity, demonstrating that shorter micropiles with smaller slenderness ratios are less effective in load distribution.

2. Effect of Water–Cement Ratio (W/C):

- As the W/C ratio increases from 0.3 to 0.55, there is a noticeable reduction in the load-bearing capacity across all slenderness ratios.
- At $W/C = 0.3$, the pile shows the highest overall performance, especially for $L/D = 14$, where loads above 5886 N are achieved at vertical displacement of about 4-5 mm.
- As the W/C ratio increases to 0.4, there is a decrease in load-bearing performance. For example, the maximum load for $L/D = 14$ reduces to around 4905 N, and the settlement tends to be smaller for the same applied loads.
- At $W/C = 0.55$, the performance declines further, with the maximum load for $L/D = 14$ dropping to below 3924 N. This confirms that a higher water–cement ratio weakens the grout, resulting in lower strength and stiffness, and consequently reducing the micropile's ability to support heavier loads.

3. Load–Settlement Behavior:

- The load–settlement curves for each L/D ratio exhibit a non-linear behavior. Initially, the piles show a rapid increase in load capacity with small deflections, but as deflection increases, the rate of load capacity gain slows down.
- For W/C = 0.3, the increase in load capacity is more pronounced, especially for L/D = 14. However, as the W/C ratio increases, the curves become flatter, indicating less load-carrying improvement as deflection increases.

4. Comparison Across W/C Ratios:

- The results clearly show that W/C = 0.3 provides the best overall performance, allowing micropiles to carry higher loads at greater deflections, especially for L/D = 12 and L/D = 14.
- W/C = 0.4 shows intermediate performance, while W/C = 0.55 exhibits the lowest load capacity across all slenderness ratios.
- The diminishing performance as W/C increases can be attributed to the reduction in grout strength due to the higher water content, which reduces the effectiveness of the micropile in bearing loads.

5. Derived mathematical model:

The derived relationship provides a comprehensive tool for predicting the load capacity of micropiles based on their geometric properties and grout composition. By incorporating both linear and non-linear terms, as well as interaction effects between displacement, slenderness ratio, and water-cement ratio, this model offers a more accurate representation of pile behavior under different conditions. Engineers can use this equation to optimize pile design, ensuring that piles are both cost-effective and capable of supporting the required loads.

$$Q = [-94.12 - 18.89 * d + 39.18 * \left(\frac{L}{D}\right) - 176.23 * \left(\frac{W}{C}\right) - 23.18 * d^2 - 1.8 * \left(\frac{L}{D}\right)^2 + 20.13 * d * \left(\frac{L}{D}\right) - 88.29 * d * \left(\frac{W}{C}\right)] * 9.81$$

6. Final observations:

- The slenderness ratio L/D plays a dominant role in enhancing load capacity, especially for lower W/C ratios, indicating that longer piles are more effective at distributing load into the soil.
- Maintaining a lower W/C ratio, particularly around 0.3, is critical for maximizing the load-bearing performance of piles, as higher W/C ratios lead to a significant reduction in both strength and stiffness.

References

- [1] F. Lizzi, ‘The pali radice (root piles)’ symposium on soil and rock improvement techniques including geotextiles reinforced earth and modern piling Methods Bangkok D3’, 1982.

- [2] C. Plumelle, 'Improvement of the bearing capacity of soil by inserts of group and reticulated micro piles', in *Proceedings*, 1984, pp. 83–89.
- [3] I. Juran, D. A. Bruce, A. Dimillio, and A. Benslimane, 'Micropiles: the state of practice. Part II: design of single micropiles and groups and networks of micropiles', <https://doi.org/10.1680/gi.1999.030301>, vol. 3, no. 3, pp. 89–110, Jun. 2015, doi: 10.1680/GI.1999.030301.
- [4] G. Sabini and G. Sapio, 'Behaviour of small diameter piles under axial load', *X ICSMFE*, vol. 2, pp. 823–828, 1981.
- [5] F. Schlosser and I. Juran, 'Design parameters for artificially improved soils', 1981, *Br Geotech Soc*. Accessed: Oct. 14, 2024. [Online]. Available: <https://nyuscholars.nyu.edu/en/publications/design-parameters-for-artificially-improved-soils>
- [6] F. LIZZI, 'RETICULATED ROOT PILES TO CORRECT LANDSLIDES', 1978.
- [7] F. LIZZI, 'THE "RETICOLO DI PALI RADICE" (RETICULATED ROOT PILES) FOR THE IMPROVEMENT OF SOIL RESISTANCE. PHYSICAL ASPECTS AND DESIGN APPROACHES', 1983.
- [8] N. SOLIMAN and G. MUNFAKH, 'Foundations on drilled and grouted mini piles : A case history', pp. 363–369, 1988.
- [9] M. W. O'Neil and R. F. Pierry, 'Behaviour of Mini-Grouted piles used in of the International Conference on Piling and Deep Foundations', 1989, *London*.
- [10] W. H. Ting and R. Nithiaraj, 'Underpinning a Medium-Rise Building with Micropiles-A Case History', *GEOTECHNICAL ENGINEERING*, vol. 31, no. 2, pp. i–i, 2000.
- [11] D. A. Bruce, 'Small-diameter cast-in-place elements for load-bearing and in situ earth reinforcement', *Ground control and improvement*, PP Xanthakos, LW Abramson, and DA Bruce, eds., Wiley Interscience, New York, 1994.
- [12] H. Hirayama, 'A unified base bearing capacity formula for piles', *Soils and foundations*, vol. 28, no. 3, pp. 91–102, 1988.
- [13] Shamsheer. Prakash and H. D. . Sharma, 'Pile foundations in engineering practice', p. 734, 1990, Accessed: Nov. 28, 2024. [Online]. Available: https://books.google.com/books/about/Pile_Foundations_in_Engineering_Practice.html?hl=ar&id=3ePSnCRi5kUC
- [14] N. H. I. FHWA, 'Micropile design and construction–reference manual. Federal Highway Administration-National Highway Institute (FHWA NHI). US Department of Transportation, McLean, Va. Publication No', FHWA NHI-05-039, 2005.
- [15] B. Sharma, S. Zaheer, and Z. Hussain, 'Experimental Model for Studying the Performance of Vertical and Batter Micropiles', *American Society of Civil Engineers (ASCE)*, Feb. 2014, pp. 4252–4264. doi: 10.1061/9780784413272.412.
- [16] Y. Huang, E. L. Hajduk, D. S. Lipka, and J. C. Adams, 'Micropile Load Testing and Installation Monitoring at the CATS Vehicle Maintenance Facility', pp. 1–10, Oct. 2007, doi: 10.1061/40902(221)28.
- [17] J. R. Wolosick, 'Ultimate Micropile Bond Stresses Observed during Load Testing in Clays and Sands', pp. 12–22, Mar. 2009, doi: 10.1061/41021(335)2.
- [18] S. Alampalli and V. Peddibotla, 'High capacity piles', *Proc. Innovations in Found. Const.*, vol. 52, no. 2, pp. 61–69, Jun. 1972, doi: 10.3208/SANDF.37.2_61.
- [19] A. J. Lutenegger, 'Low Energy Compacted Concrete Grout Micropiles', pp. 146–157, Jan. 2004, doi: 10.1061/40713(2004)6.
- [20] S. Bhardwaj and S. K. Singh, 'Experimental Study on Model Micropiles under Oblique Pullout Loads', pp. 610–621, May 2014, doi: 10.1061/9780784413449.059.